

## BEM and FEM analysis of fluid–structure interaction in a double tank



J. Ravnik<sup>a</sup>, E. Strelnikova<sup>b,\*</sup>, V. Gnitko<sup>b</sup>, K. Degtyarev<sup>b</sup>, U. Ogorodnyk<sup>b</sup>

<sup>a</sup> University of Maribor, Faculty of Mechanical Engineering, Smetanova ulica, 17, SI-2000 Maribor, Slovenia

<sup>b</sup> A N. Podgorny Institute of Mechanical Engineering Problems of the Ukrainian Academy of Sciences, 2/10, D. Pozharsky str., Kharkov 61023, Ukraine

### ARTICLE INFO

#### Article history:

Received 6 October 2015

Received in revised form

18 January 2016

Accepted 17 February 2016

#### Keywords:

Fluid–structure interaction

Baffles

Free vibrations

Boundary and finite element methods

### ABSTRACT

In this paper we present a fluid–structure interaction analysis of shell structures with compartments partially filled with a liquid. The compound shell was a simplified model of a fuel tank. The shell is considered to be thin and Kirghoff–Lave linear theory hypotheses are applied. The liquid is ideal and incompressible. Its properties and the filling levels may be different in each compartment. The shell vibrations coupled with liquid sloshing under the force of gravity were considered. The shell and sloshing modes were analysed simultaneously. The coupled problem is solved using a coupled BEM and FEM in-house solver. The tank structure is modeled by FEM and the liquid sloshing in the fluid domain is described by BEM. The method relies on determining the fluid pressure from the system of singular integral equations. For its numerical solution, the boundary element method was applied. The boundary of the liquid computational domain is discretized by nine-node boundary elements. The quadratic interpolation of functions and linear interpolation of flux are involved. The natural frequencies were obtained for the cylindrical double tank with two compartments.

© 2016 Elsevier Ltd. All rights reserved.

### 1. Introduction

Fuel tanks and containers for storage of oil and other dangerous liquids are extensively used in different engineering areas such as aerospace industry, chemical and oil–gas industry, power machine building and transport. These reservoirs operate under excess process loads, and are filled with oil, flammable or toxic liquids.

The influences of both shell and fluid on each other must not be neglected in stress–strength analysis of these structural elements. Therefore, the interaction between the sloshing liquid and the shell structure has been a challenging field of research in many engineering applications.

Liquid sloshing is an interesting physical phenomenon of enormous practical interest that has far reaching applications in a wide field of technologies and engineering disciplines. It occurs in moving tanks with contained liquid masses such as rocket tanks, marine and space vehicles as well as in seismically excited storage tanks, dams, reactors, and nuclear vessels. The book of Ibrahim [1] gives a detailed summary of the theory and fundamentals of sloshing under widely various conditions.

Many different types of model tests at different scales and with different objectives were proposed and performed in the last years in this research area. Since the launch of the early high-efficient

rockets in 1957, controlling liquid fuel slosh during a vehicle launch has been a major design concern. Moreover, with today's large and complex spacecrafts, a substantial mass of fuel is required to place them into orbit and to perform orbital maneuvers. The mass of fuel contained in the tanks of a geosynchronous satellite amounts to approximately 40% of its total mass as it was shown by Sidi [2]. When the fuel tanks are only partially filled, large quantities of fuel move inside the tanks under translational and rotational accelerations and generate the fuel slosh dynamics. Slosh control of propellant is a significant challenge to spacecraft stability. Robinson et al. [3] and Space Exploration Technologies Corp. [4] proved that in several cases mission failure has been attributed to slosh-induced instabilities.

As the propellant level decreases throughout a mission, the effects of sloshing forces on the remaining fuel become more prominent. When the fuel tank is full or nearly so, the fuel lacks the open space to slosh. But, in the latter stages of the mission, when most of the fuel has been consumed, the fuel has sufficient volume to slosh and possibly disturb the flight trajectory. This sloshing can ultimately lead to wobble in a spinning spacecraft and self-amplifying oscillations that can result in failure of separate parts or the whole structure. The dynamics of a fluid interacting with the walls of its container is complicated and challenging to predict. The effects of sloshing are significant and in some cases remain prominent even when the propellant volume

\* Corresponding author.

E-mail address: [estrel@ipmach.kharkov.ua](mailto:estrel@ipmach.kharkov.ua) (E. Strelnikova).

represents only 0.3% of the total spacecraft mass as reported by Vreeburg [5].

In order to suppress sloshing a variety of methods have been proposed, simulated and tested. The effects of baffle on sloshing frequency have been studied by Biswal et al. [6]. The mathematical technique used here is based on the velocity potential function; the problem was solved using finite-element analysis.

The motion of liquid within a partially filled tank was investigated by Ranganathan et al. [7] by representing the fluid slosh through an equivalent mechanical system using a pendulum analogy model. The model parameters were computed based on inviscid fluid flow conditions and the dynamic fluid slosh forces arising due to the dynamics of the vehicle during a given maneuver were computed using the equivalent mechanical system.

Liquid sloshing in partially filled horizontal cylindrical tanks with circular cross sections is a common problem in the road transportation industry that has been extensively studied for many years [8–10]. A recent review on liquid sloshing in horizontal cylindrical tanks was presented by Hasheminejad et al. [11].

In order to restrain the fluid sloshing motion a common technique is to place additional sub-structures called baffles or separators within the tank, as it was demonstrated by Strandberg [8]. Thus, we must consider the problem of sloshing in so-called double tanks or tanks with the compartments.

The issue of suppression of sloshing behavior using baffles goes back to late 50s when lots of experimental and theoretical studies were concerned with the effect of baffles on the sloshing in fuel containers of space vehicles [12,13].

Since then, numerous authors have tackled the subject. Strandberg [8] performed an experimental investigation of dynamic performance and stability of horizontal circular tank. He also studied the overturning limit for half-full elliptical containers with various baffle configurations and concluded that the vertical baffle must be preferred in comparison with the un-baffled or horizontally baffled elliptical container. Evans et al. [14] used the method of eigenfunction series to explore the effect of a thin vertical baffle in a fluid-filled rectangular tank on fluid frequencies. This technique was subsequently extended to consider circular containers having internal baffles by Watson et al. [15]. A mathematical model was developed for the ship rolling motion with free surface liquids on board by Armenio et al. [16]; numerical and experimental results for a rectangular tank with a vertical bottom-mounted internal baffle were presented here. Modaressi-Tehrani et al. [17] used the FLUENT software to develop a three-dimensional nonlinear model of a partly-filled cylindrical tank with and without baffles to investigate the significance of resulting destabilizing forces and moments. The main objective of Sidi [2] was to analyze multi-excitation effects on a cylinder divided by plate on two compartments on the base using BEM and FEM numerical analysis. Diverse multi-exciting forces were applied on this base plate with different frequencies whereas, independently calculated results were superimposed to provide consolidated result.

A semi-analytical approach was presented by Wang [18,19] to obtain both natural frequencies and vibration modes of ideal liquid sloshing and the sloshing response of liquid in a rigid cylindrical container with multiple annual rigid baffles subjected to lateral excitations. The complicated liquid domain was divided into several simple sub-domains. Based on the superposition principle, the analytical solutions of the liquid velocity potential corresponding to each liquid sub-domain were obtained by the method of separation of variables. Analysis of transient lateral slosh in a partially-filled cylindrical tank with different designs of longitudinal partial baffles was performed by Kolaei et al. [20] by using a coupled multimodal and boundary-element method. Shahravi et al. [21] proposed a method to model the influence of different

baffle geometries on liquid sloshing. It has been shown that the natural frequencies and the dynamic response of the liquid are drastically changed if the free liquid surface in a cylindrical container is covered with some rigid structural parts. Liquid sloshing in a cubic tank with multiple baffles was investigated numerically in detail by Xue et al. [22] under different external excitation frequencies. Wachowski et al. [23] noted that tank sloshing mainly occurs due to maneuvers like stop-and-go traffic or parking; sloshing that is generated depends on the tank geometry, filling level, fuel type and excitation and it leads to the three different types of slosh noise: splash, hit and clonk. Kandasamy et al. [24] presented the analysis of effectiveness of different baffle designs in limiting the maneuver-induced transient sloshing in a partly-filled tank. Xue et al. [25] and Eswaran et al. [26] performed the theoretical and experimental research devoted to sloshing problems in a rectangular liquid tank with a perforated baffle. The horizontal ring and vertical blade baffles and their damping effects were investigated by Maleki et al. [27]. After comparing the tank without baffles with the one with baffles, Yan et al. found [28] that the sloshing mode, basic frequencies and free surface shape are all affected by the baffles.

Range of applicability of the linear fluid slosh theory for predicting sloshing vibrations and stability of tank was described by Ibrahim [1], Armenio et al. [16] and Yan et al. [28]. In these papers it was shown that the linear slosh model yields more accurate prediction of dynamic slosh than the pendulum models and it is significantly more computationally efficient than the nonlinear CFD model. Liu et al. [29] adopted finite difference method which solves Navier–Stokes equations to study 2D and 3D viscous and inviscid liquid sloshing in rectangular tanks and verified the results with the linear analytical solution and experimental data. It was demonstrated by [18,28,29] that suppositions about inviscid, incompressible liquid and its irrotational flow are applicable for small amplitude excitations where the wave breaking and the influence of non-linearities do not influence the overall system response significantly. This model can also be used for initial design calculations and in engineering problems regarding to cargo vehicle dynamics, dynamics of road tankers, vehicle fuel tank described in [9,20,23,24,27–29]. So we accept these suppositions hereinafter.

Modeling of sloshing in tanks and reservoirs, as an imprecise and complicated engineering event, has an unfinished evolution history. The above review clearly indicates that there exists a massive body of literature on liquid sloshing in rectangular or upright cylindrical containers with various baffle configurations. With respect to all the numerical work, which has been done, it is fair to say that there is still no fully efficient numerical method to deal with the sloshing in fluid–structure interactions in two-compartmental tanks. Indeed, it appears that, from computational point of view, it is very difficult to account for all the different physical effects at the same time.

In this work, we propose a method of fluid–structure interaction analysis for tanks with compartments partially filled with liquids, that allows us to include elasticity of shell walls, different liquid properties in each compartment, gravity force and to estimate influence of these factors on frequencies of tank vibration. In this paper the free vibration analysis of an elastic cylindrical shell is coupled with liquid sloshing. We use the combination of reduced finite and boundary element methods. The analysis consists of several stages where each stage represents a separate task. The frequencies and modes of empty shell vibrations are defined in the first stage. Displacement vector, that is the solution of the hydrodynamic problem, is sought as a linear combination of natural modes of empty shell. We define the frequencies and free vibrations modes of fluid-filled elastic shell without including the force of gravity. Then, we obtain the frequencies and free

vibrations modes of liquid in rigid shell under force of gravity. Two latter problems are solved using reduced BEM. Then we come to the problem of coupled analysis of liquid sloshing and structural vibrations.

**2. Problem statement**

Let us consider the coupled problem of a shell structure with two compartments partially filled with the liquid (Fig. 1). In this study, we consider the cylindrical shell with elastic bottom and baffle. The contained liquid is assumed inviscid and incompressible. We suppose that liquid properties and filling levels may be different in each compartment.

Hereinafter we denote the surface of an empty tank as  $S$ . The domains occupied with liquid we denote as  $\Omega_1$  and  $\Omega_2$  for first and second compartments. The wetted boundaries of these domains are  $S_1$  and  $S_2$  and free surfaces are  $S_{10}$  and  $S_{20}$  accordingly.

Suppose that the flow induced by vibrations of the shell are irrotational and consider small shell and fluid vibrations. Let the unknown vector-function of the shell displacements be denoted by  $\mathbf{U}$ . A system of governing equations of motion of elastic shell with the liquid in the operator form is given by

$$\mathbf{L}(\mathbf{U}) + \mathbf{M}(\ddot{\mathbf{U}}) = \mathbf{P} \tag{1}$$

where  $\mathbf{L}$ ,  $\mathbf{M}$  are operators of elastic and mass forces of the shell;  $\mathbf{U} = (u_1, u_2, u_3)$  is the displacement vector,  $\mathbf{P}$  is the liquid pressure.

The liquid densities in compartments are  $\rho_1$  and  $\rho_2$  respectively. Filling levels in compartments will be denoted as  $h_1$  and  $h_2$ . Please note that the fluid velocity potential  $\Phi$  satisfies the Laplace equation.

For velocity potential  $\Phi$  we obtain a mixed boundary value problem for Laplace equation in double domain  $\Omega_1 \cup \Omega_2$ . Hereinafter we denote the normal displacement component of tank structure as  $w$ , i.e.  $w = (\mathbf{U}, \mathbf{n})$ .

Then the kinematical boundary condition of continuous fluid motion on the wetted shell surface  $S$  can be represented as

follows:

$$\frac{\partial \Phi}{\partial \mathbf{n}} = \frac{\partial w}{\partial t}$$

where  $\mathbf{n}$  is an external unit normal to wetted surface,  $S = S_1 \cup S_2$ .

Let functions  $\zeta_1(t, x, y, z)$  and  $\zeta_2(t, x, y, z)$  describe the shapes and positions of free surfaces in the first and second compartments. These surfaces are denoted as  $S_{10}, S_{20}$  in Fig. 1. On free surfaces, the following formulae for pressure components are valid [1]:

$$p_1 - p_{10} = -\rho_1 \left( \frac{\partial \Phi}{\partial t} + g \zeta_1 \right); \quad p_2 - p_{20} = -\rho_2 \left( \frac{\partial \Phi}{\partial t} + g \zeta_2 \right).$$

Here  $g$  is the gravity acceleration.

To determine the function  $\Phi$  the following boundary value problem in the double domain  $\Omega_1 \cup \Omega_2$  is formulated with free-surface boundary conditions (kinematical and dynamical) and non-penetration condition on wetted parts [11,30]:

$$\Delta \Phi = \frac{\partial^2 \Phi}{\partial x^2} + \frac{\partial^2 \Phi}{\partial y^2} + \frac{\partial^2 \Phi}{\partial z^2} = 0; \quad \frac{\partial \Phi}{\partial \mathbf{n}} \Big|_S = \frac{\partial w}{\partial t}; \quad \frac{\partial \Phi}{\partial \mathbf{n}} \Big|_{S_{10}} = \frac{\partial \zeta_1}{\partial t}; \quad \frac{\partial \Phi}{\partial \mathbf{n}} \Big|_{S_{20}} = \frac{\partial \zeta_2}{\partial t}; \quad \frac{\partial \Phi}{\partial t} + g \zeta_1 \Big|_{S_{10}} = 0; \quad \frac{\partial \Phi}{\partial t} + g \zeta_2 \Big|_{S_{20}} = 0 \tag{2}$$

Here  $w$  indicates the normal component of shell deflection.

So it is necessary to solve Eqs. (1) and (2) simultaneously including the boundary conditions for shell structure and using the next presentation for the dynamical components of the liquid pressure on tank walls:

$$p_l = (\mathbf{P}, \mathbf{n}) = \begin{cases} -\rho_1 \frac{\partial \Phi}{\partial t}; & M \in \partial \Omega_1, \\ -\rho_2 \frac{\partial \Phi}{\partial t}; & M \in \partial \Omega_2 \end{cases}$$

It leads to the system of differential equations.

**3. Mode superposition method**

We will seek the natural modes of vibration for a double tank interacting with the fluid in the form

$$\mathbf{u} = \sum_{k=1}^N c_k \mathbf{u}_k \tag{3}$$

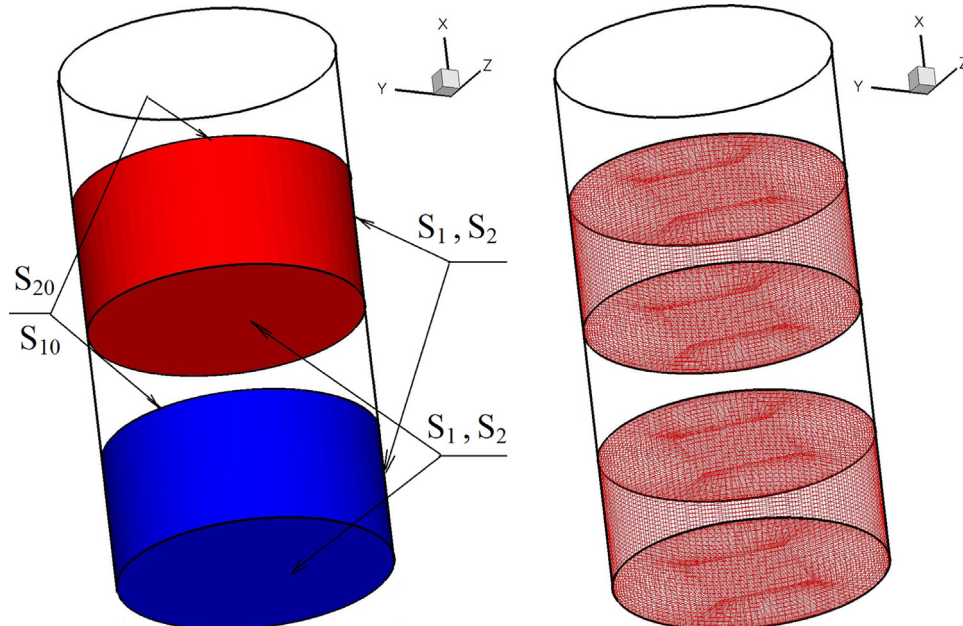


Fig. 1. Fluid-filled double tank. The right panel show the computational mesh used for BEM solution of inviscid fluid flow.

Here functions  $\mathbf{u}_k(x, y, z)$  are natural vibration modes of the empty tank,  $c_k(t)$  are unknown factors depending on time  $t$  only. The own modes of an empty tank are defined on the cylindrical part of shell structure, its bottom and baffle.

Let us note that the following relationships are fulfilled [31]:

$$\mathbf{L}(\mathbf{u}_k) = \Omega_k^2 \mathbf{M}(\mathbf{u}_k), (\mathbf{M}(\mathbf{u}_k), \mathbf{u}_j) = \delta_{kj}, (\mathbf{L}(\mathbf{u}_k), \mathbf{u}_j) = \Omega_k^2 \delta_{kj} \quad (4)$$

where  $\Omega_k$  is the  $k$ -th frequency of the empty shell vibrations. The above relations show that the empty shell's modes of vibration must be orthonormalized with respect to the mass matrix.

Let also introduce the denominations

$$\mathbf{u}_j = \begin{cases} \mathbf{u}_j^1; & M \in S_1, \\ \mathbf{u}_j^2; & M \in S_2. \end{cases}$$

We will hereinafter seek the function  $\Phi$  as a sum of two potentials  $\Phi = \Phi_1 + \Phi_2$ . For the potential  $\Phi_1$  we define the frequencies and free vibrations modes of fluid-filled elastic shell without including the force of gravity. To determine  $\Phi_1$  we have to use the series

$$\Phi_1 = \sum_{k=1}^N \dot{c}_k \phi_{1k}$$

Here time-dependent factors  $c_k(t)$  were defined in (3). To determine  $\phi_{1k}$  we have the following boundary value problems:

$$\nabla^2 \phi_{1k} = 0; \quad \left. \frac{\partial \phi_{1k}}{\partial \mathbf{n}} \right|_S = w_k; \quad \phi_{1k}|_{S_{10}} = 0; \quad \phi_{1k}|_{S_{20}} = 0 \quad (5)$$

Here  $w_k$  indicates the normal component of the mode  $\mathbf{u}_k$ , i.e.  $w_k = (\mathbf{u}_k, \mathbf{n})$ .

It follows from Eq. (5) that the problem for the double domain is reduced to boundary value problems for two single domains

$$\nabla^2 \phi_{1k}^i = 0; \quad M \in \Omega_i; \quad \left. \frac{\partial \phi_{1k}^i}{\partial \mathbf{n}} \right|_{S_i} = w_k^i; \quad M \in \Omega_i; \quad \phi_{1k}^i|_{S_{i0}} = 0 \quad (6)$$

Here  $S = S_1 + S_2$ ;  $S_1, S_2$  are wetted parts of double tank surface of two compartments,  $S_{10}, S_{20}$  are free surfaces,  $w_k^1, w_k^2$  are normal component of the mode  $\mathbf{u}_k$  in the first and second compartments. Functions  $\phi_{1k}^1$  and  $\phi_{1k}^2$  are solutions of problems (6) for  $i=1$  and  $i=2$  accordingly.

Then for potential  $\Phi_1$  we obtain the next representation:

$$\Phi_1 = \begin{cases} \sum_{k=1}^{M_1} \dot{c}_k \phi_{1k}^1, & M \in \partial\Omega_1, \\ \sum_{k=1}^{M_2} \dot{c}_k \phi_{1k}^2, & M \in \partial\Omega_2. \end{cases}$$

For evaluating the potential  $\Phi_2$  we will obtain the frequencies and free vibrations modes of liquid in rigid shell under force of gravity. Before determining the function  $\Phi_2$ , let us consider the auxiliary problems for two fluid-filled compartments [30]

$$\nabla^2 \Psi_i = 0; \quad \left. \frac{\partial \Psi_i}{\partial \mathbf{n}} \right|_{S_i} = 0; \quad \left. \frac{\partial \Psi_i}{\partial \mathbf{n}} \right|_{S_{i0}} = \frac{\partial \zeta_i}{\partial t}; \quad \frac{\partial \Psi_i}{\partial t} + g \zeta_i|_{S_{i0}} = 0 \quad (7)$$

Considering harmonic vibrations and omitting indexes, we have supposed that  $\Psi = \psi e^{i\omega t}$ . Therefore, we have eigenvalue problems to solve in each compartment. Let us denote as  $\phi_{2k}^1, \chi_k^1, \phi_{2k}^2, \chi_k^2$  the modes and frequencies for first and second compartments respectively. We have differentiated the fourth equation in relationship (7) with respect to  $t$  and then substituted the expression for  $\frac{\partial \zeta_i}{\partial t}$  from the third one of Eq. (7). Thus, the following relations are valid on free surfaces of compartments:

$$\frac{\partial \phi_{2k}^1}{\partial \mathbf{n}} = \frac{(\chi_k^1)^2}{g} \phi_{2k}^1|_{S_{10}}; \quad \frac{\partial \phi_{2k}^2}{\partial \mathbf{n}} = \frac{(\chi_k^2)^2}{g} \phi_{2k}^2|_{S_{20}},$$

Then the potential  $\Phi_2$  is represented in the form

$$\Phi_2 = \begin{cases} \sum_{k=1}^{M_1} b_k \phi_{2k}^1, & M \in \partial\Omega_1, \\ \sum_{k=1}^{M_2} d_k \phi_{2k}^2, & M \in \partial\Omega_2. \end{cases}$$

Here  $M_1$  and  $M_2$  are quantities of sloshing modes in first and second compartments.

Finally, the total velocity potential  $\Phi$  takes the form

$$\Phi = \begin{cases} \sum_{k=1}^N \dot{c}_k \phi_{1k}^1 + \sum_{k=1}^{M_1} b_k \phi_{2k}^1, & M \in \Omega_1, \\ \sum_{k=1}^N \dot{c}_k \phi_{1k}^2 + \sum_{k=1}^{M_2} d_k \phi_{2k}^2, & M \in \Omega_2. \end{cases} \quad (8)$$

When functions  $\phi_{1k}^1, \phi_{1k}^2, \phi_{2k}^1, \phi_{2k}^2$  are known, we have the next relationship to determine the pressure on the wetted parts:

$$p_l = \begin{cases} -\rho_1 \left( \sum_{k=1}^N \ddot{c}_k \phi_{1k}^1 + \sum_{k=1}^{M_1} \ddot{b}_k \phi_{2k}^1 \right); & M \in \partial\Omega_1, \\ -\rho_2 \left( \sum_{k=1}^N \ddot{c}_k \phi_{1k}^2 + \sum_{k=1}^{M_2} \ddot{d}_k \phi_{2k}^2 \right); & M \in \partial\Omega_2. \end{cases}$$

The total potential  $\Phi$  satisfies the Laplace equation and non-penetration boundary condition (first and second relations in Eq. (2)). These results allow us to obtain the following expressions for free-surface shapes in both compartments as following:

$$\zeta_1 = \sum_{k=1}^N c_k \frac{\partial \phi_{1k}^1}{\partial \mathbf{n}} + \sum_{k=1}^{M_1} b_k \frac{\partial \phi_{2k}^1}{\partial \mathbf{n}}, \quad \zeta_2 = \sum_{k=1}^N c_k \frac{\partial \phi_{1k}^2}{\partial \mathbf{n}} + \sum_{k=1}^{M_2} d_k \frac{\partial \phi_{2k}^2}{\partial \mathbf{n}} \quad (9)$$

Noted that  $\Phi$  also satisfies the conditions

$$\left. \frac{\partial \Phi}{\partial \mathbf{n}} \right|_{S_{10}} = \frac{\partial \zeta_1}{\partial t}, \quad \left. \frac{\partial \Phi}{\partial \mathbf{n}} \right|_{S_{20}} = \frac{\partial \zeta_2}{\partial t}$$

as a result of representations (8) and (9).

Satisfying the conditions

$$\frac{\partial \Phi}{\partial t} + g \zeta_1|_{S_{10}} = 0; \quad \frac{\partial \Phi}{\partial t} + g \zeta_2|_{S_{20}} = 0$$

on free surfaces  $S_{10}, S_{20}$ , one can obtain the next equalities

$$\sum_{k=1}^N \ddot{c}_k \phi_{1k}^1 + \sum_{k=1}^{M_1} \ddot{b}_k \phi_{2k}^1 + g \left( \sum_{k=1}^N c_k \frac{\partial \phi_{1k}^1}{\partial \mathbf{n}} + \sum_{k=1}^{M_1} b_k \frac{\partial \phi_{2k}^1}{\partial \mathbf{n}} \right) = 0; \quad (10)$$

$$\sum_{k=1}^N \ddot{c}_k \phi_{1k}^2 + \sum_{k=1}^{M_2} \ddot{d}_k \phi_{2k}^2 + g \left( \sum_{k=1}^N c_k \frac{\partial \phi_{1k}^2}{\partial \mathbf{n}} + \sum_{k=1}^{M_2} d_k \frac{\partial \phi_{2k}^2}{\partial \mathbf{n}} \right) = 0 \quad (11)$$

To these equations we need to add the Eq. (1) written in the following form:

$$\mathbf{L} \left( \sum_{k=1}^N c_k(t) \mathbf{u}_k \right) + \mathbf{M} \left( \sum_{k=1}^N \dot{c}_k(t) \mathbf{u}_k \right) = (\mathbf{P}, \mathbf{n}) \quad (12)$$

Please note that  $\phi_{1k}^i|_{S_{i0}} = 0, i = 1, 2$ . Using expressions for  $\Phi, p_l, \zeta_1(t, x, y, z)$  and  $\zeta_2(t, x, y, z)$ , substituting them into (eqs. (10)-12) and performing dot products, we have obtained the following system of ordinary differential equations

$$c_j(t) \Omega_j^2 + \ddot{c}_j(t) = -\rho_1 \left( \sum_{k=1}^N \ddot{c}_k(t) (\phi_{1k}^1, \mathbf{u}_j^1) + \sum_{k=1}^{M_1} \ddot{b}_k(t) (\phi_{2k}^1, \mathbf{u}_j^1) \right) - \quad (13)$$

$$-\rho_2 \left( \sum_{k=1}^N \ddot{c}_k(t) (\phi_{1k}^2, \mathbf{u}_j^2) + \sum_{k=1}^{M_2} \ddot{d}_k(t) (\phi_{2k}^2, \mathbf{u}_j^2) \right);$$

$$\alpha_{1j}\ddot{b}_j(t) + g \sum_{k=1}^N c_k(t) \left( \frac{\partial \phi_{1k}^1}{\partial n}, \phi_{2j}^1 \right) + \alpha_{1j} b_j(t) (\chi_j^1)^2 = 0; j = 1, \dots, M_1; M \in S_{10};$$

$$\alpha_{2j}\ddot{d}_j(t) + g \sum_{k=1}^N c_k(t) \left( \frac{\partial \phi_{1k}^1}{\partial n}, \phi_{2j}^1 \right) + \alpha_{2j} d_j(t) (\chi_j^1)^2 = 0; j = 1, \dots, M_2; M \in S_{20}.$$

Here we have

$$\alpha_{kj} = (\phi_{2j}^k, \phi_{2j}^k); \quad k = 1, 2.$$

In doing so we have multiplied the Eq. (12) by functions  $u_k$ , and (Eqs. (10) and 11) by functions  $\phi_{2k}^1$  and  $\phi_{2k}^2$  respectively.

To evaluate the free vibration frequencies we will seek the solution of system (13) in the form

$$b_k(t) = B_k \exp(i\omega t); \quad c_k(t) = C_k \exp(i\omega t); \quad d_k(t) = D_k \exp(i\omega t).$$

Then we obtain the next eigenvalue problem to define frequencies  $\omega$  and modes  $X = (C_k, B_k, D_k)^T$ :

$$(-\omega^2 M + G)X = 0$$

where

$$M = \begin{pmatrix} E + \rho_2 P & \rho_2 B^1 & \rho_2 B^2 \\ 0 & E & 0 \\ 0 & 0 & E \end{pmatrix}; \quad G = \begin{pmatrix} \Omega & 0 & 0 \\ gG^1 & H_1 & 0 \\ gG^2 & 0 & H_2 \end{pmatrix}$$

$$G^i = \{g_{kj}^i\}; \quad g_{kj}^i = \left( \frac{\partial \phi_{1k}^i}{\partial n}, \phi_{2j}^i \right); \quad k = 1, M_i; \quad j = 1, N$$

$$B^i = \{b_{jk}^i\}; \quad b_{jk}^i = (\phi_{2k}^i, u_j^i); \quad j = 1, \dots, N; \quad k = 1, \dots, M_i$$

Here  $\Omega, H_1, H_2$  are diagonal matrixes with squares of frequencies as diagonal elements for free vibrations of empty tank, liquid sloshing in first and second tank compartments accordingly.

#### 4. BEM solution of velocity potential $\Phi_1$

The velocity potential  $\phi_{1k}$  for the  $k$ -th eigen-frequency of tank oscillation is governed by the Laplace equation

$$\nabla^2 \phi_{1k} = 0 \tag{14}$$

with boundary conditions (5), where the wall normal displacement is  $w = u_z$  at the bottom and  $w = u_r$  at the cylindrical part of tank shell structure in cylindrical coordinate system.

In the framework of the boundary element method the Eq. (14) may be rewritten into the following integral form in the following way [32]

$$c(M_0)\phi_{1k}(M_0) + \int_{\Gamma} \phi_{1k}(M) (\vec{\nabla} u^*, \vec{n}) dS = \int_{\Gamma} (q_k, \vec{n}) u^* dS; \quad (q_k, \vec{n}) = \frac{\partial \phi_{1k}}{\partial n}; \quad \Gamma = S_i \cup S_{i0} \tag{15}$$

where  $M_0$  is the source or collocation point,  $\vec{n}$  is a unit normal to the boundary, pointing out of the domain and  $u^*$  is the fundamental Laplace solution  $u^* = (4\pi \cdot |M - M_0|)^{-1}$ ;  $c(M_0)$  is the geometrical factor defined as  $c(M_0) = \alpha/4\pi$ , where  $\alpha$  is an inner angle with origin in collocation point  $M_0$ .

The boundary of the computational domain is discretized by boundary elements  $\Gamma = \sum_b \Gamma_b$ . Each boundary element consists of 9 nodes for quadratic interpolation of functions and 4 nodes for linear interpolation of flux. Velocity potential is interpolated over the boundary elements as  $\phi_{1k} = \sum L_i \phi_{k,i}$ . The flux is interpolated over the boundary elements as  $q_k = \sum L_i q_{k,i}$ , using discontinuous linear interpolation scheme, avoiding the definition problem in corner points. By applying the described interpolation, the

following form of Eq. (15) can be written as:

$$c(M_0)\phi_{1k}(M_0) + \sum_b \int_{\Gamma_b} L_i \phi_{k,i} (\vec{\nabla} u^*, \vec{n}) dS = \sum_b \int_{\Gamma_b} (L_i q_{k,i}, \vec{n}) u^* dS$$

with  $i$  denoting the node number. After the following integral are calculated,

$$[H] = \int_{\Gamma} L_i (\vec{\nabla} u^*, \vec{n}) dS; \quad [G] = \int_{\Gamma} L_i u^* dS$$

the Eq. (15) is transformed into the matrix form

$$c(M_0)\phi_{1k}(M_0) + [H]\{\phi_{1k}\} = [G]\{q_k\} \tag{16}$$

The square brackets in Eq. (16) denote integral matrixes and each source point yields one row in these matrices. Gaussian quadrature algorithm was used for calculation the integrals, which were evaluated in local coordinate system. A weighted summation of up to 48 integration points on each coordinate axis was used. In the case when the source point is located within the element, where integration takes place, such integrals are singular. The calculation of the singular integral and the estimation of the free coefficient  $c(M_0)$  are performed indirectly. Rigid body movement  $\phi = 1, q = 0$  is considered and thus the sum of all  $[H]$  matrix elements for each source point is zero. This fact is used to indirectly estimate the diagonal terms of the  $[H]$  matrix and avoid integration of the singular integrals. After application of boundary conditions the system may be solved for unknown boundary values of velocity potential or its normal derivative. This method is based on the BEM fluid flow solver developed by Ravnik et al. [33].

#### 5. BEM solution of velocity potential $\Phi_2$

To determine the potential  $\Phi_2$  we have to obtain auxiliary functions  $\psi_k$ . Let us denote by  $\psi_{1k}$  the values of  $\psi_k$  on the wetted surface  $S_1$  and by  $\psi_{0k}$  the values of  $\psi_k$  on the free surface  $S_0$ . We will seek harmonic functions  $\phi_{2k}$  as the sums of potentials of single and double layers [32], i.e., we will use the direct boundary element method formulation.

Using the BEM direct formulation and skipping for convenience the index  $k$ , we can write the following system of singular integral equations

$$2\pi\psi_1 + \iint_{S_1} \psi_1 \frac{\partial}{\partial n} \left( \frac{1}{r} \right) dS_1 - \frac{\kappa^2}{g} \iint_{S_0} \psi_0 \frac{1}{r} dS_0 + \iint_{S_0} \psi_0 \frac{\partial}{\partial z} \left( \frac{1}{r} \right) dS_0 = 0,$$

$$-\iint_{S_1} \psi_1 \frac{\partial}{\partial n} \left( \frac{1}{r} \right) dS_1 - 2\pi\psi_0 + \frac{\kappa^2}{g} \iint_{S_0} \psi_0 \frac{1}{r} dS_0 = 0.$$

Suppose that

$$\psi = \psi(r, z) \cos \alpha \theta \tag{17}$$

We obtain for each harmonic the following system of singular integral equations

$$\iint_{S_1} \psi \frac{\partial}{\partial n} \left( \frac{1}{r(P, P_0)} \right) dS_1 = \int_r \psi(z) \Theta(z, z_0) r(z) dz d\Gamma, \tag{18}$$

$$\iint_{S_0} \psi \left( \frac{1}{r(P, P_0)} \right) dS_0 = \int_0^R \psi(\rho) \Phi(P, P_0) \rho d\rho.$$

Here kernels  $\Theta(z, z_0)$  and  $\Phi(P, P_0)$  are defined as

$$\Theta(z, z_0) = \frac{4}{\sqrt{a+b}} \left\{ \frac{1}{2r} \left[ \frac{r^2 - r_0^2 + (z_0 - z)^2}{a-b} E_\alpha(k) - F_\alpha(k) \right] n_r + \frac{z_0 - z}{a-b} E_\alpha(k) n_z \right\}$$

$$\Phi(P, P_0) = \frac{4}{\sqrt{a+b}} F_\alpha(k).$$

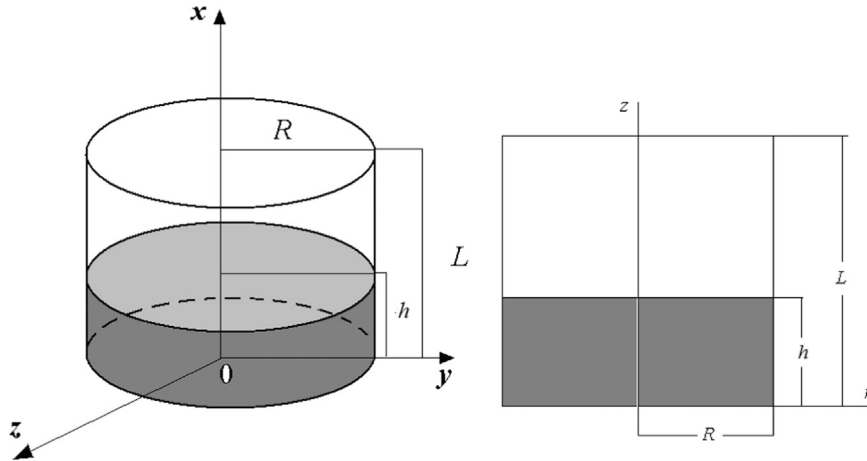


Fig. 2. Cylindrical shell partially filled with a liquid.

To reach the numerical solution of the system of singular integral equations, the boundary element method with constant approximation of unknown density on elements was used [30]. Integration by the fluid volume is reduced to integrals along the shell meridian and along the radius of the liquid free surface. It is the basic advantage of our method based on the combination of boundary integral equations method, FEM, BEM and expansion into Fourier series. It should be noted that the only FEM analysis requires 3D modeling to solve this coupled problem. That leads to essentially more computer time and it does not allow using effectively such methods in computer monitoring problems.

Let introduce the next integral operators:

$$\begin{aligned}
 A\psi_1 &= 2\pi\psi_1 + \iint_{S_1} \psi_1 \frac{\partial}{\partial n} \left( \frac{1}{|P-P_0|} \right) dS_1; B\psi_0 = \iint_{S_0} \psi_0 \frac{1}{r} dS_0; C\psi_0 \\
 &= \iint_{S_0} \psi_0 \frac{\partial}{\partial z} \left( \frac{1}{r} \right) dS_0 \\
 D\psi_1 &= -\iint_{S_1} \psi_1 \frac{\partial}{\partial n} \left( \frac{1}{|P-P_0|} \right) dS_1; F\psi_0 = \iint_{S_0} \psi_0 \frac{1}{r} dS_0
 \end{aligned} \tag{19}$$

Then the boundary value problem (18) takes the form

$$A\psi_1 = \frac{\kappa^2}{g} B\psi_0 - C\psi_0; \quad P_0 \in S_1; \quad D\psi_1 = 2\pi E\psi_0 - \frac{\kappa^2}{g} F\psi_0; \quad P_0 \in S_0$$

After excluding function  $\psi_1$  from these relations, we obtain a below stated eigenvalue problem; its solution gives the natural modes and frequencies of liquid sloshing in rigid tank

$$(DA^{-1}C + E)\psi_0 - \lambda(DA^{-1}B + F)\psi_0 = 0; \quad \lambda = \frac{\chi^2}{g}.$$

Numerical solution of the system of integral 18(18) and evaluation of integral operators in 19(19) was obtained by BEM with constant approximation of unknowns  $\phi$  and  $q$  inside elements.

It would be noted that internal integrals in (Eqs. (18) and 19) are complete elliptic integrals of first and second kinds. As the first kind elliptic integrals are non-singular, one can successfully use standard Gaussian quadratures for their numerical evaluation. For second kind elliptic integrals we have used the approach based on the characteristic property of the arithmetic geometric mean AGM ( $a, b$ ) (see [34]). The above-mentioned characteristic property consists in following:

$$\int_0^{\frac{\pi}{2}} \frac{d\theta}{\sqrt{a^2 \cos^2 \theta + b^2 \sin^2 \theta}} = \frac{\pi}{2AGM(a, b)}.$$

To define AGM( $a, b$ ) there exist the simple Gaussian algorithm, described below

$$a_0 = a; \quad b_0 = b; \quad a_1 = \frac{a_0 + b_0}{2}; \quad b_1 = \sqrt{a_0 b_0}; \dots a_{n+1} = \frac{a_n + b_n}{2};$$

$$b_{n+1} = \sqrt{a_n b_n}; \dots$$

$$AGM(a, b) = \lim_{n \rightarrow \infty} a_n = \lim_{n \rightarrow \infty} b_n. \tag{20}$$

It is a very effective method to evaluate the elliptic integrals of the second kind. Convergence  $\varepsilon = |a_n - b_n| < 10^{-8}$  achieved after 6 iterations (namely,  $n = 6$  in (20)).

We have the effective numerical procedures for evaluation of inner integrals, but integral (Eqs. (18) and 19) involve external integrals of logarithmic singularities and thus the numerical treatment of these integrals will also have to take into account the presence of this integrable singularity. Here integrands are distributed strongly non-uniformly over the element and standard integration quadratures fail in accuracy. Thus we treat these integrals numerically by special Gauss quadratures [32,35] and applying technique proposed by Naumenko and Strelnikova [36].

In order to obtain the second set of basic functions we consider the liquid sloshing in the rigid cylindrical shell. We use the analytical solution [1] of this problem that can be expressed in the form

$$\begin{aligned}
 \frac{\chi_k^2}{g} &= \frac{\mu_k}{R} \tanh\left(\mu_k \frac{h}{R}\right), \quad k = 1, 2, \dots; \quad \phi_{2k} \\
 &= J_0\left(\frac{\mu_k r}{R}\right) \cosh\left(\frac{\mu_k z}{R}\right) \cosh^{-1}\left(\frac{\mu_k h}{R}\right)
 \end{aligned} \tag{21}$$

in order to test the proposed numerical algorithm. Here  $h$  is the filling level and  $R$  is the radius of cylindrical shell.

Noted that in 21(21) values  $\mu_k$  are roots of the equation

$$\frac{dJ_0(x)}{dx} = 0,$$

where  $J_0(x)$  is Bessel function of first kind,  $\chi_k, \phi_{2k}$  are frequencies and modes of liquid sloshing in the rigid cylindrical shell.

Consider the circular cylindrical shell with a flat bottom and having the following parameters: the radius is  $R = 1$  m, the thickness is  $h_s = 0.01$  m, the length  $L = 2$  m, the fluid density  $\rho_l = 1000$  kg/m<sup>3</sup>. The filling level of the fluid is  $h = 0.8$  m. The geometry of the tank is shown in Fig. 2.

The numerical solution was obtained by using BEM as it was described beforehand. In the present numerical simulation we used 60 boundary elements along the bottom, 60 elements along the wetted cylindrical part and 100 elements along the radius of the free surface. Fig. 3 shows the first three modes of liquid sloshing at the free surface in the rigid cylindrical shell.

Table 1 below provides the numerical values of the first five natural frequencies of liquid sloshing for nodal diameter  $\alpha = 0$ . The obtained numerical results are compared with those received using formulae (21).

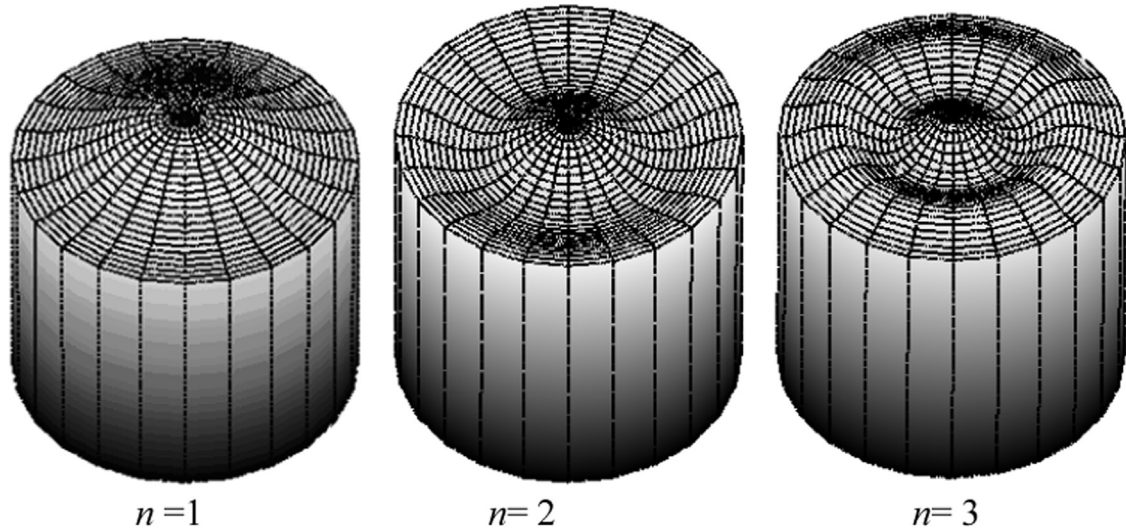


Fig. 3. Axisymmetrical modes of liquid sloshing in cylindrical shell.

Table 1  
Comparison of analytical and numerical results

	$n=1$	$n=2$	$n=3$	$n=4$	$n=5$
BEM	3.815	7.019	10.180	13.333	16.480
Analytical solution	3.815	7.016	10.173	13.324	16.470

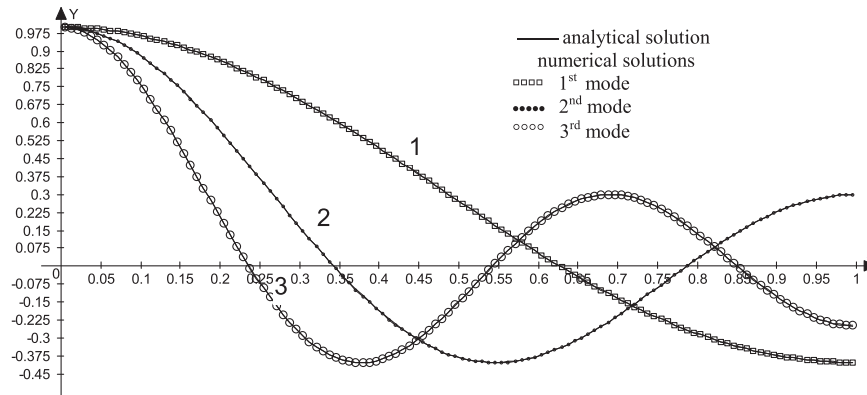


Fig. 4. Numerically (points) and analytically (lines) obtained modes.

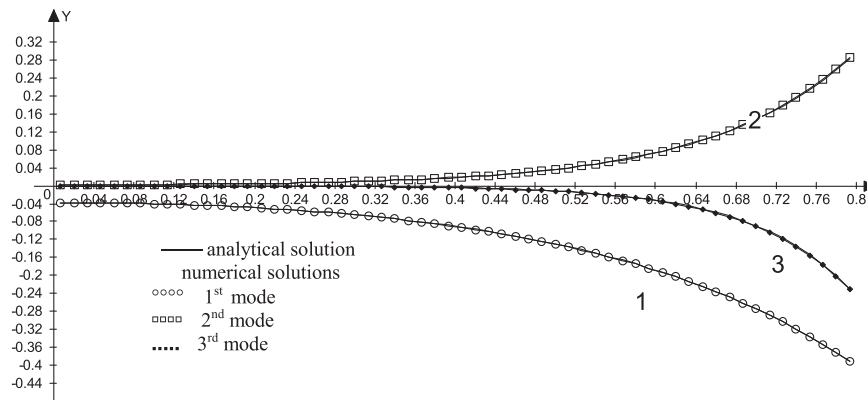


Fig. 5. Sloshing modes on the vertical wall.

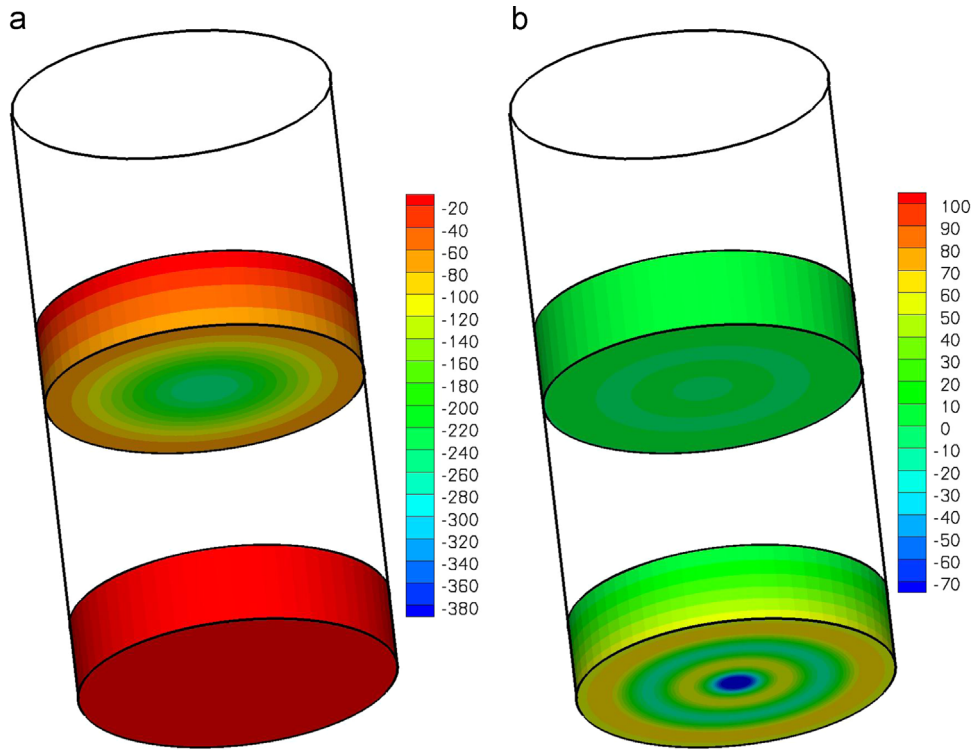


Fig. 6. Axially symmetric modes of vibration of the double tank at filling level  $h=0.75$  m, (a)  $n=1$  (b)  $n=2$ .

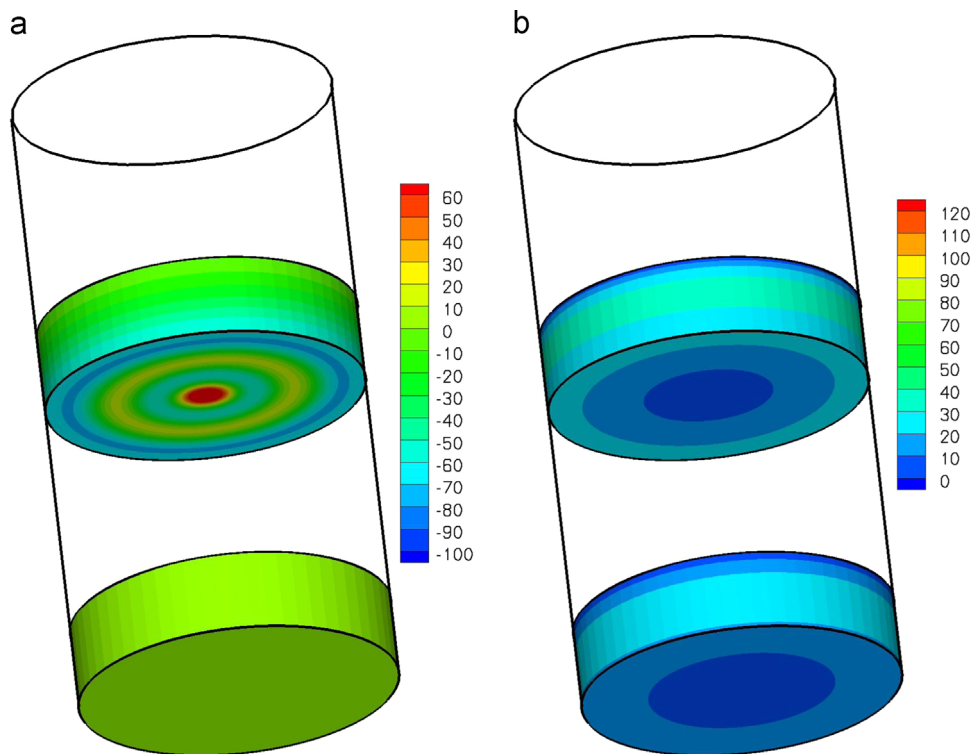


Fig. 7. Axially symmetric modes of vibration of the double tank at filling level  $h=0.75$  m, (a)  $n=8$  (b)  $n=10$ .

Figs. 4 and 5 also demonstrate good agreement between numerical and analytical data.

In Fig. 4 the distribution of first three axisymmetrical sloshing modes on the free surface is shown. The solid lines denote modes obtained by analytical expression (21) at  $z=h$ . Fig. 5 demonstrates

the distribution of these modes on the rigid vertical wall of the shell. The lines pointed with circles and squares denote numerical solutions. Numbers 1,2,3 correspond to the first, second and third modes of liquid sloshing. It would be noted that the accuracy  $\varepsilon = 10^{-4}$  has been achieved here.

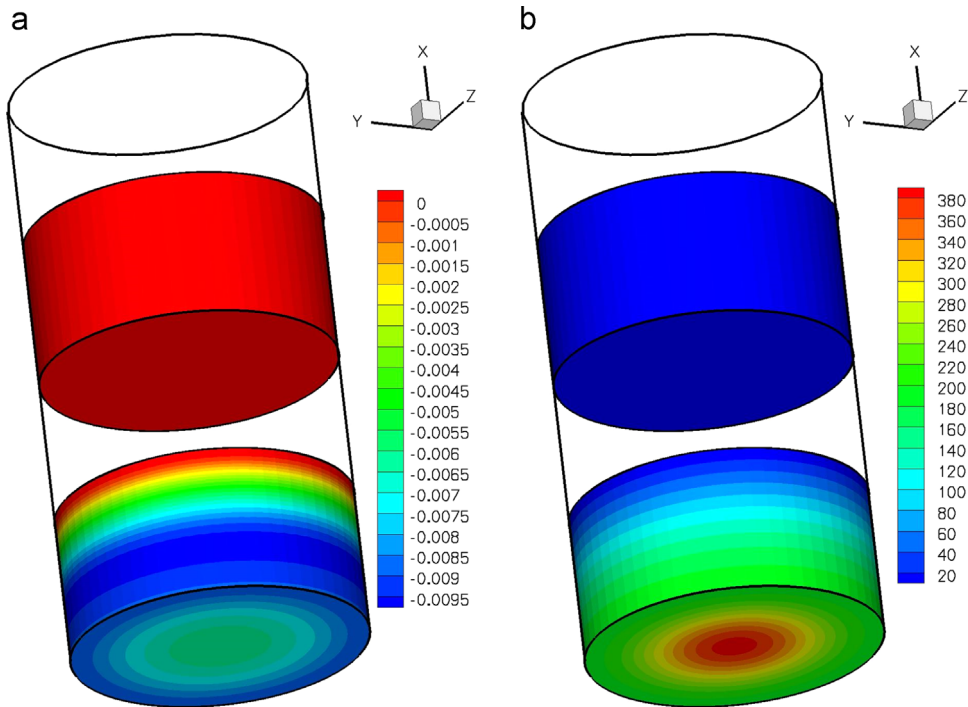


Fig. 8. Axially symmetric modes of vibration of the double tank at filling level  $h=1.5$  m, (a)  $n=1$  (b)  $n=2$ .

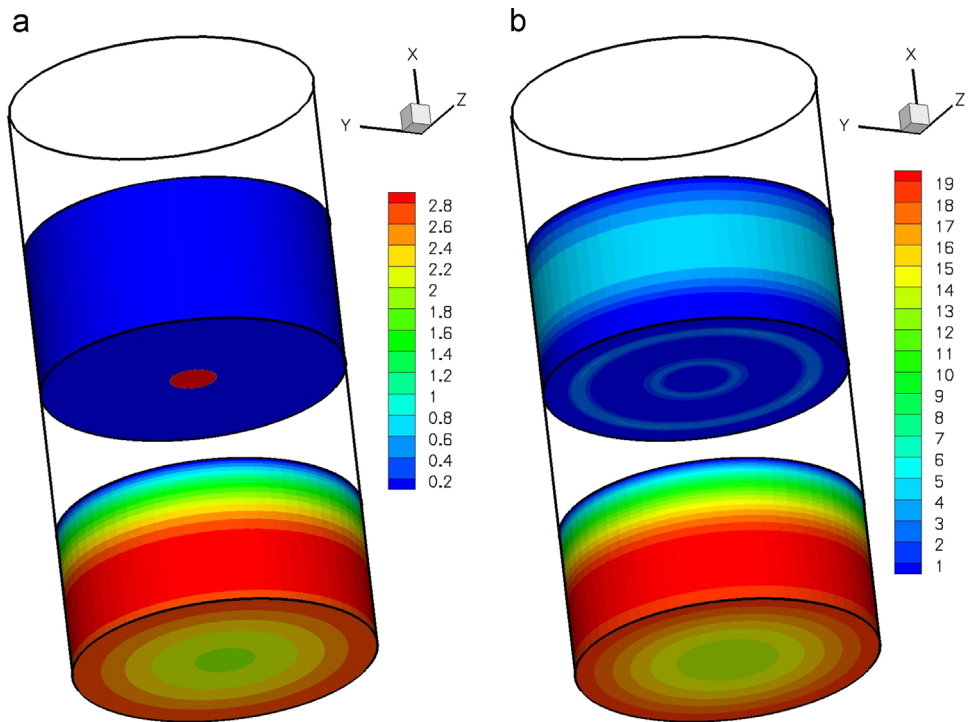


Fig. 9. Axially symmetric modes of vibration of the double tank at filling level  $h=1.5$  m, (a)  $n=8$  (b)  $n=10$ .

The obtained results have demonstrated the good agreement between numerical and analytical data. So the effectiveness of proposed method has been proved.

### 6. Numerical results of double tank vibration analysis

Here we analyze the effects of installing the baffle, the filling level and coupling effects of the shell structure and sloshing vibrations on the frequencies and modes of the double tank.

Let us consider the double tank with compartments partially filled with the fluid. The geometry of the tank is shown in Fig. 1 and the parameters are following: the radius is  $R = 1.5$  m, the thickness is  $h_s=0.01$  m, the length  $L=6$  m, Young's modulus  $E=2 \cdot 10^5$  MPa, Poisson's ratio  $\nu=0.3$ , the material's density is  $\rho=7800$  kg/m<sup>3</sup>, the fluid density in both compartments  $\rho_1=\rho_2=1000$  kg/m<sup>3</sup>. The filling level of the fluid is denoted as  $h$  (Fig. 1). It is equal in both compartments  $h_1=h_2=h$ .

In numerical simulations we consider different values as  $h=0.75$  m,  $h=1.5$  m and  $h=2.75$  m. The shell is assumed to be

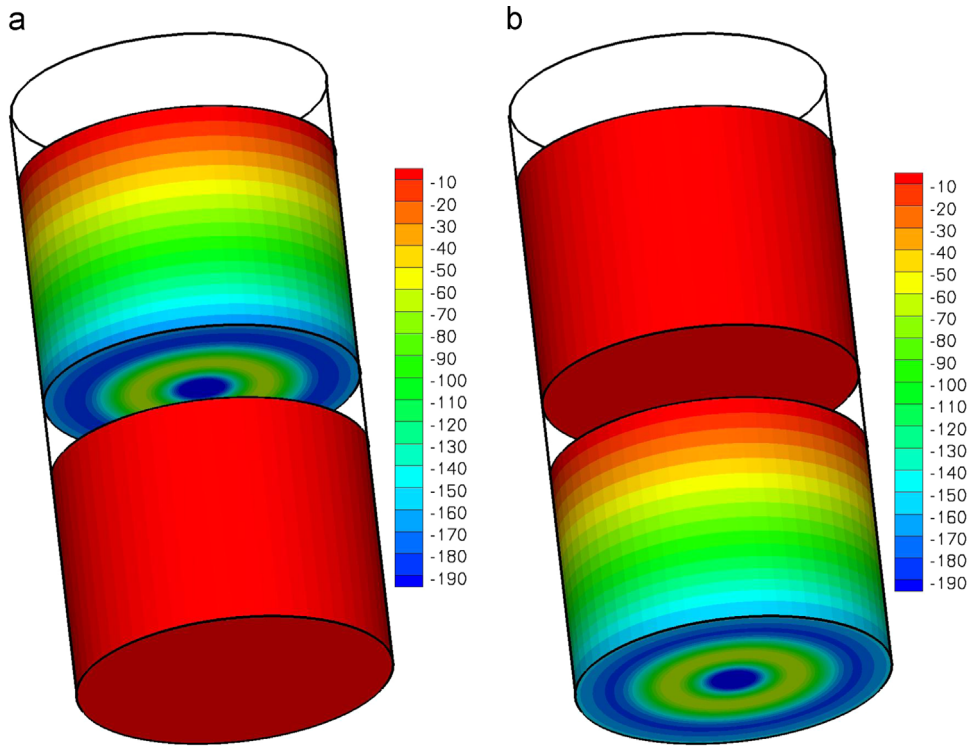


Fig. 10. Axially symmetric modes of vibration of the double tank at filling level  $h=2.75$  m, (a)  $n=1$  (b)  $n=2$ .

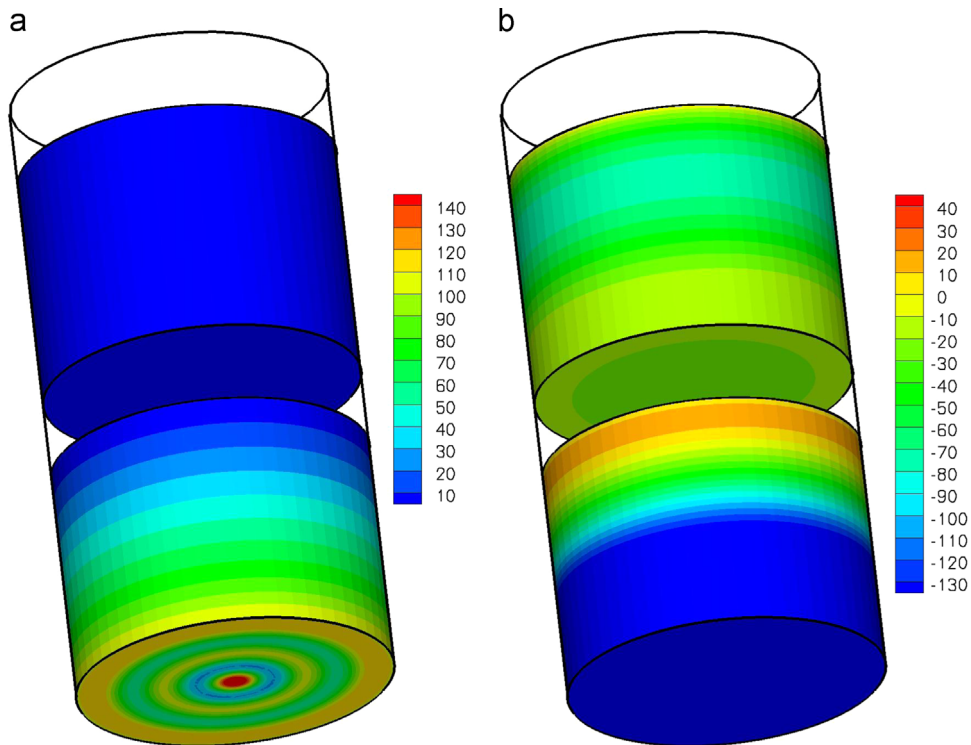


Fig. 11. Axially symmetric modes of vibration of the double tank at filling level  $h=2.75$  m, (a)  $n=8$  (b)  $n=10$ .

pin-connected over its contour and boundary conditions are following:  $u_r = u_z = u_\theta = 0$  to  $z=0$  and  $r=R$ . The modes and frequencies of empty shell were obtained using FEM as it was described by Ventsel et al. [31].

The axisymmetric forms of vibrations were under consideration. The number of natural modes of empty shell was equal to 20.

Here in FEM we used 20 cubic elements along bottom and baffle and 20 elements along cylindrical part.

Functions  $\phi_{1k}$  were calculated by method developed in [33] and based on BEM. The simulation of top and bottom compartments was done separately. Boundary conditions were obtained by interpolation of structural analysis. The computational mesh

**Table 2**  
Frequencies of empty and fluid-filled tanks without baffles

Empty elastic tank	$h = 1.5 \text{ m}$			$h = 3.0 \text{ m}$			$h = 5.50 \text{ m}$		
	$n_S$	$n_L$	Fluid-filled tank	$n_S$	$n_L$	Fluid-filled tank	$n_S$	$n_L$	Fluid-filled tank
		1	5.0010		1	5.0024		1	5.0048
		2	6.7709		2	6.7709		2	6.7709
		3	8.1568		3	8.1568		3	8.1568
		4	9.1334		4	9.1334		4	9.1334
		5	10.378		5	10.378		5	10.378
34.47	1	1,2	29.243	1	1,2	22.661	1	1,2	15.432
134.2	2,1		102.863	2,1		89.719	2,1		79.719
300.7	3,2		272.63	3,2,1		238.42	3,2,1		178.42
408.2	4,3,2		407.69	4,3		404.00	4,3		392.00

**Table 3**  
Frequencies of the double tank vibrations.

$n$	$C_1$	$C_2$	$B_1$	$B_2$	Empty tank	Fluid-filled tank
1	0.01	0.00	0.97	0.00		5.00103
2	0.00	0.01	0.00	0.97		5.00173
3	0.01	0.00	0.97	0.00		6.77016
4	0.00	0.02	0.00	0.97		6.78022
5	0.82	0.24	0.21	0.01	33.4493	7.03487
6	0.28	0.85	0.01	0.31	34.4767	7.29735
7	0.06	0.00	0.95	0.00		8.15270
8	0.00	0.08	0.00	0.947		8.15270
23	0.82	0.54	0.23	0.01	130.329	39.39860
24	0.51	0.85	0.01	0.31	134.221	40.76115
25	0.91	0.2	0.07	0.01	292.025	107.45330
26	0.2	0.947	0.028	0.08	300.718	110.89764
27	0.82	0.50	0.21	0.01	516.812	223.56725
28	0.52	0.85	0.01	0.31	533.886	224.72695

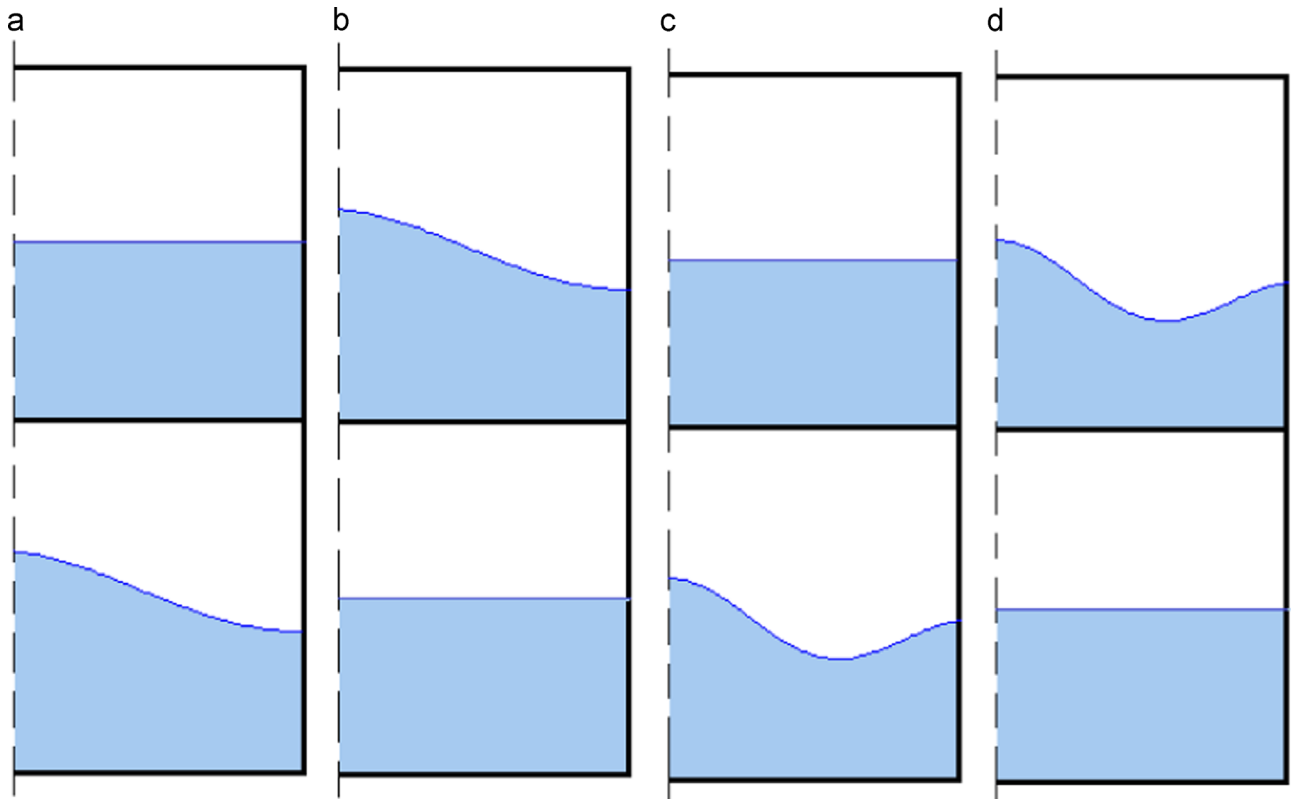


**Fig. 12.** Axially symmetric sloshing modes of vibration of the double tank, (a) 1st mode (b) 2nd mode (c) 3rd mode (d) 4th mode.

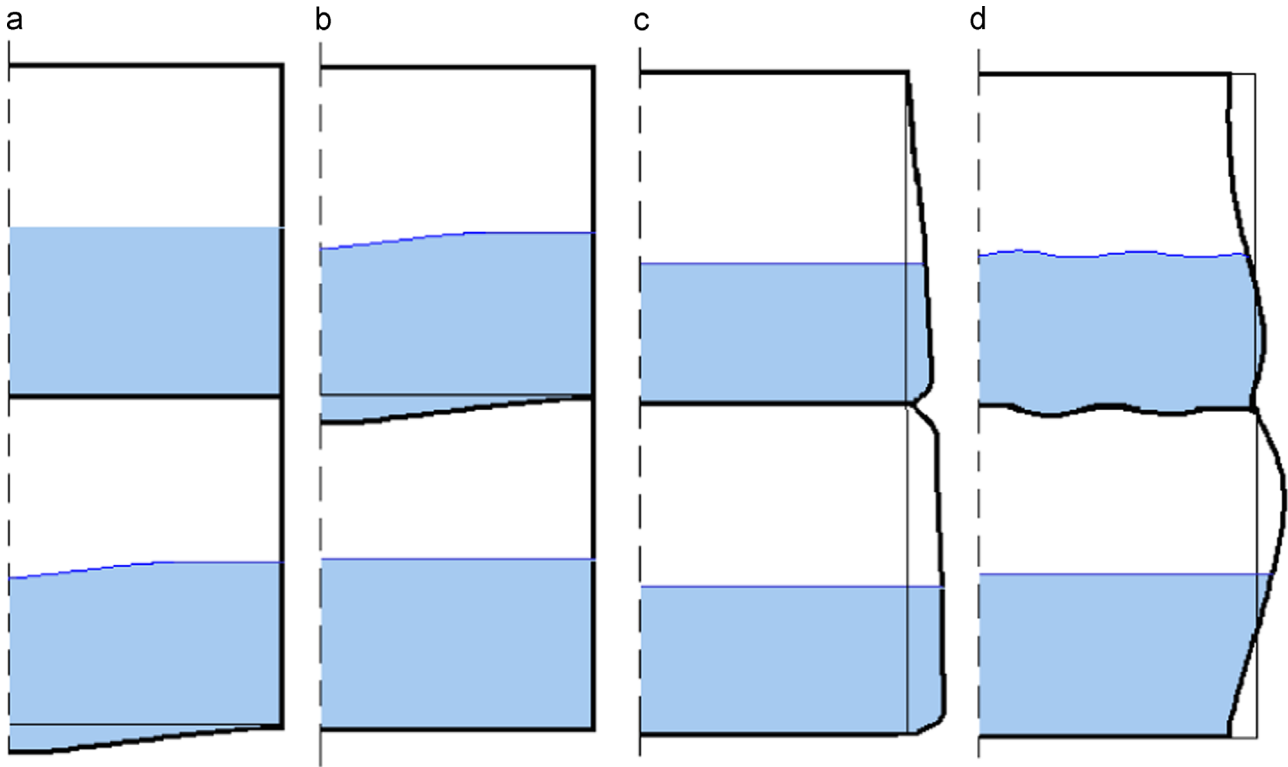


Fig. 13. Axially symmetric coupled modes of vibration of the double tank, (a) 5th mode (b) 6th mode (c) 23rd mode (d) 28th mode.

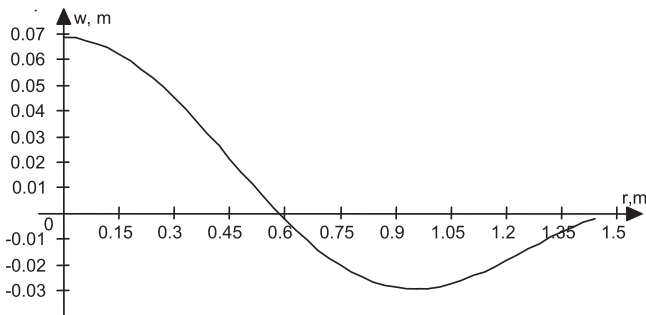


Fig. 14. Distribution of the baffle deflection over the tank radius for 4th sloshing mode.



Fig. 15. Distribution of the cylindrical wall deflection over the tank length for 23rd coupled mode.

(Fig. 1) had 3584 elements with 14,338 function nodes and 14,336 flux nodes. Here we used quadratic interpolation of functions and linear interpolation of flux.

In present numerical simulation to obtain functions  $\phi_{2k}$  we used 60 linear boundary elements along bottom, 60 linear elements along wetted cylindrical part and 60 linear boundary elements along the radius of free surface. The numbers of eigen liquid sloshing modes were  $M_1=M_2=20$  for both compartments. The sloshing modes were obtained by method described above.

Figs 6–11 demonstrate the mode shapes of liquid vibration corresponding to 1st, 2nd, 8th and 10th modes of the liquid in the double tank at different filling levels. These results were obtained by method described in [33].

For comparison we consider the cylindrical shell without baffle but with the same dimensions and material properties. We suppose that filling level of the liquid in this shell was equal to  $h = h_1 + h_2$ .

Table 2 provides the numerical values of natural frequencies of vibrations for empty and fluid-filled cylindrical tanks without baffle in increasing order. Here coefficients  $n_s, n_l$  indicate numbers of modes of the shell and liquid involved in coupled vibrations.

Table 3 provides the numerical values of the natural frequencies of vibrations for empty and fluid-filled double tank. Here coefficients  $C_1, C_2, B_1, B_2$  indicate the mode of vibration. Coefficients  $C_1, C_2$  are regarded to shell walls vibrations in first and second compartments, and coefficients  $B_1, B_2$  corresponds to modes of liquid sloshing in first and second compartments accordingly.

These results demonstrated that the frequencies of tanks with and without baffles are essentially different. Installing the baffle leads to a decrease of the frequencies of vibrations. The supposition about the spectrum separation of frequencies of the elastic shell filled with the liquid and sloshing frequencies in the rigid shell with the same geometrical characteristics and filling level as for the elastic one is not valid in presence of baffles.

Fig. 12 demonstrates the first 4 modes of the double tank vibrations at filling level  $h = 1.5$  m. These modes are predominantly sloshing ones as it was shown in Table 3. So the low frequencies correspond to liquid sloshing without deformations of the tank walls.

Fig. 13 demonstrates the coupled shell and sloshing modes at filling level  $h = 1.5$  m. The 5th mode corresponds to the coupled

liquid and bottom vibrations and 6th one corresponds to the coupled liquid and baffle vibrations. The 23rd mode is the mode of the cylindrical wall vibrations only, and the 28th mode corresponds to the coupled vibrations of cylindrical parts, the baffle and the liquid sloshing in second compartment.

Separately, distributions of the deflections of the tank baffle and cylindrical wall are displayed in Figs. 14 and 15. These results demonstrate that deformations of the tank baffle and bottom are more essentially than that of the cylindrical wall.

The results obtained here allow us to analyze the effect of baffles at the coupled liquid and shell vibrations. It has been showed that the natural frequencies of the tank structure are essentially changed at installing the baffle. It was demonstrated that the sloshing and shell vibrations can not be considered separately. Simulation results showed the effectiveness of this numerical procedure. The presented approach may be also applied to the different geometry of container

## 7. Conclusions

The numerical procedure based on the coupling finite element formulation and boundary element method is developed for numerical analysis of fluid–structure interaction for a double tank. We introduce the representation of the velocity potential as the sum of two potentials, one of them corresponds to problem of the fluid free vibrations in the rigid shell and another one corresponds to problem of elastic shell with fluid without including the gravitational component. Integration by the fluid volume is accomplished using BEM based fluid flow solver. The spectrum of frequencies for double tank was analysed.

## Acknowledgments

The authors gratefully acknowledge Professor Carlos Brebbia for his constant support and interest to our research. We are also grateful to Ukrainian and Slovenian Ministries (Grant number M/72 years 2013–2014) for our bilateral research grant “Development of fast boundary element method for fluid flow applications”.

## References

- [1] Ibrahim RA. *Liquid Sloshing Dynamics*. Cambridge: Cambridge University Press; 2005.
- [2] Sidi MJ. *Spacecraft Dynamics and Control*. New York: Cambridge University Press; 1997.
- [3] Robinson H.G.R., Hume C.R. Europa Europa I: Flight Trial of F1- 5th; June,1964.
- [4] Space Exploration Technologies Corp. Demo Flight 2 Flight Review Update; June 15, 2007.
- [5] Jan P.B. Vreeburg. Spacecraft Maneuvers and Slosh Control. *IEEE Control Systems Magazine*; 2005.
- [6] Biswal KC, Bhattacharyya SK, Sinha PK. Dynamic characteristics of liquid filled rectangular tank with baffles. *IE (I) Journal-CV* 2004;84:145–8.
- [7] Ranganathan R, Ying Y, Miles, J., Analysis of fluid slosh in partially filled tanks and their impact on the directional response of tank vehicles. *SAE Technical Paper* 10; 1993, p. 932–42.
- [8] Strandberg, L. Lateral Stability of Road Tankers VTI Report No. 138A; 1978. p. 1.
- [9] Romero JA, Hildebrand R, Martínez M, Ramírez O, Fortanell JM. Natural sloshing frequencies of liquid cargo in road tankers. *Int. J. Heavy Veh. Syst.* 2005;12:121–38.
- [10] Xu L. *Fluid Dynamics in Horizontal Cylindrical Containers and Liquid Cargo Vehicle Dynamics* (Ph.D thesis, ). Saskatchewan: University of Regina; 2005.
- [11] Hasheminejad SM, Aghabeigi M. Liquid sloshing in half-full horizontal elliptical tanks. *J Sound Vib* 2009;324:332–49.
- [12] Silveira A.M., Stephens D.G., Leonard H.W. An experimental investigation of liquid oscillation in tanks with various baffles NASA Technical Note D-715; 1961.
- [13] Abramson, H.N. *Slosh Suppression*. NASA Technical Report SP-8031, 1969.
- [14] Evans DV, McIver P. Resonant frequencies in a container with a vertical baffle. *J Fluid Mech* 1987;175:295–307.
- [15] Watson EBB, Evans DV. Resonant frequencies of a fluid container with internal bodies. *J Eng Math* 1991;25:115–35.
- [16] Armenio V, Rocca ML. On the analysis of sloshing of water in rectangular containers: numerical study and experimental validation. *Ocean Eng* 1996;23:705–39.
- [17] Modaresi-Tehrani K, Rakheja S, Stiharu I. Three-dimensional analysis of transient slosh within a partly-filled tank equipped with baffles. *Veh. Syst. Dyn.* 2007;45:525–48.
- [18] Wang JD, Lo SH, Zhou D. Liquid sloshing in rigid cylindrical container with multiple rigid annular baffles: free vibration. *J Fluids Struct* 2012;34:138–56.
- [19] Wang JD, Lo S, Zhou SH. Liquid sloshing in rigid cylindrical container with multiple rigid annular baffles: lateral vibration. *J Fluids Struct* 2013;42:421–36.
- [20] Kolaei, A., Rakheja, S., Richard, M.J. Anti-sloshing effects of longitudinal partial baffles in a partly-filled container under lateral excitation. *ASME 2014 International Mechanical Engineering Congress and Exposition V. 4A: Dynamics, Vibration, and Control Montreal, Quebec, Canada; November 14–20, 2014.*
- [21] Shahravi M, Azimi M. Effects of baffles geometry on sloshing dynamics of a viscous liquid tank. *Sci Res Essays* 2012;7(47):4092–9.
- [22] Xue Mi-An, Ji, Zheng, Lin P. Numerical Simulation of Sloshing Phenomena in Cubic Tank with Multiple Baffles. *Journal of Applied Mathematics* 2012;21 Article ID 245702.
- [23] Wachowski1 C., Biermann1 J.-W., Schala R. Approaches to analyse and predict slosh noise of vehicle fuel tanks. In: *Proceedings of the 24th International Conference on Noise and Vibration engineering*, p. 4401–417.
- [24] Kandasamy T, Rakheja S, Ahmed AKW. An analysis of baffles designs for limiting fluid slosh in partly filled tank trucks. *Open Transp J* 2010;4:23–32.
- [25] Xue Mi-an, Lin Peng-zhi, Zheng Jin-hai, Ma Yu-xiang, Yuan Xiao-li, Nguyen Viet-Thanh. Effects of perforated baffle on reducing sloshing in rectangular tank: experimental and numerical study. *China Ocean Eng.* 2013;27(5):615–28.
- [26] Eswaran M, Saha UK, Maity D. Effect of baffles on a partially filled cubic tank: Numerical simulation and experimental validation. *J Comput Struct* 2009;87:198–205.
- [27] Maleki A, Ziyaeifar M. Sloshing damping in cylindrical liquid storage tanks with baffles. *J Sound Vib* 2008;311(1–2):372–85.
- [28] Yan Jin, Yu Hong Liang. The free sloshing modal analysis of liquid tank with baffles. *Adv Mater Res* 2011;10:347–53.
- [29] Liu D, Lin P. A numerical study of three-dimensional liquid sloshing in tanks. *J. Comput. Phys.* 2008;227:3921–39.
- [30] Gnitko V, Marchenko U, Naumenko V, Strelnikova E. Forced vibrations of tanks partially filled with the liquid under seismic load. *WIT Trans Model Simul* 2011;52:285–96.
- [31] Ventsel E, Naumenko V, Strelnikova E, Yeseleva E. Free vibrations of shells of revolution filled with a fluid. *Eng Anal Bound Elem* 2010;34:856–62.
- [32] Brebbia CA, Telles JCF, Wrobel LC. *Boundary Element Techniques*. Berlin and New York: Springer-Verlag; 1984.
- [33] Ravnik J, Škerget L, Žunic Z. Velocity-vorticity formulation for 3D natural convection in an inclined enclosure by BEM. *Int J Heat Mass Transfer* 2008;51:4517–27.
- [34] Cox D.A. *The Arithmetic-Geometric Mean of Gauss*. *L'Enseignement Mathématique*, t. 30; 1984. p. 275–330.
- [35] Stroud AH, Secrest D. *Gaussian Quadrature Formulas*. Englewood Cliffs, N.J: Prentice-Hall; 1966.
- [36] Naumenko VV, Strelnikova HA. Singular integral accuracy of calculations in two-dimensional problems using boundary element methods. *Eng Analysis Bound Elem* 2002;26:95–8.